Topological Floquet Spectrum in Three Dimensions via a Two-Photon Resonance

Netanel H. Lindner[1,2], Doron L. Bergman[2], Gil Refael[2], Victor Galitski [3,4,5]
1) Institute of Quantum Information, California Institute of Technology, Pasadena, CA 91125, USA.
2) Department of Physics, California Institute of Technology, Pasadena, CA 91125, USA.
3) Center for Nanophysics and Advanced Materials, Department of Physics, University of Maryland, College Park, Maryland 20742-4111, USA
4) Joint Quantum Institute, Department of Physics, University of Maryland, College Park, Maryland 20742, USA. and
5) Kavli Institute for Theoretical Physics, University of California Santa Barbara, CA 93106-4030

A recent theoretical work [Nature Phys., **7**, 490 (2011)] has demonstrated that external non-equilibrium perturbations may be used to convert a two-dimensional semiconductor, initially in a topologically trivial state, into a Floquet topological insulator. Here, we develop a non-trivial extension of these ideas to three-dimensional systems. In this case, we show that a two-photon resonance may provide the necessary twist needed to transform an initially unremarkable band structure into a topological Floquet spectrum. We provide both an intuitive, geometrical, picture of this phenomenon and also support it by an exact solution of a realistic lattice model that upon irradiation features single topological Dirac modes at the two-dimensional boundary of the system. It is shown that the surface spectrum can be controlled by choosing the polarization and frequency of the driving electromagnetic field. Specific experimental realizations of a three-dimensional Floquet topological insulator are proposed.

Three dimensional topological insulators exhibit a variety of novel electronic properties. The most prominent of these are surface states, whose dispersion is that of massless, chiral two dimensional Dirac fermions. A dispersion with an odd number of Dirac cones is unique to surfaces of three dimensional systems, as it is otherwise precluded by the Fermion doubling theorem. Such surface states were observed recently by angular resolved emission spectroscopy in a variety of new materials, such as Bi_xSb_{1-x} alloys, Bi_2Te_3,and Bi_2Se_3 [1–3]. The unusual structure of the surface states is predicted to lead to unique response properties of these materials. Among these is the axion magnetoelectric response [4, 5], which arises when the Dirac cone is gapped due to breaking of time reversal symmetry, for example by application of a perpendicular magnetic field. This response is akin to having a fractional $\nu = 1/2$ Hall response at the surface of the material. Moreover, the surface states of topological insulators play a crucial role in proposals for quantum interference devices. Most notable of these is the possibility to realize and manipulate Majorana Fermions [6], which have important applications for topological quantum computing.

The topological behavior of electrons is emerging as a promising resource, and therefore it is imperative that we understand all ways to induce it. In this manuscript we explore the possibility of dynamically inducing a three dimensional topological spectrum, surface states included, starting with a trivial (non-topological) bulk insulator. The idea of inducing topological order with periodic modulations of a Hamiltonian was explored in Refs. 7–10. The Floquet spectrum of a periodically driven system was shown to exhibit a variety of topological phases, including one that exhibits a single Dirac cone [7]. Physical examples include graphene which is expected to exhibit a quantum Hall effect when subjected to radiation [9, 11, 12], and spin-orbit coupled semiconductor heterostructure (such as HgTe/CdTe wells), which can be turned from trivial to topological using microwave-teraHertz radiation [10], and vice versa [13].

In this manuscript we demonstrate how a "time reversal invariant" three dimensional topological spectrum can be induced in trivial insulators using electro-magnetic radiation. This problem is a non-trivial generalization of its 2D analog [10]. Roughly speaking, a topologically trivial band structure can be turned topological by mixing the valence and conduction bands, for instance by radiative transitions. In 3D, the radiation has to be carefully tailored such that it produces a non-vanishing band inversion matrix element in a closed 2D surface in momentum space, and, as we shall see, must obey additional topological and symmetry constraints. The polarization and frequency of the driving electromagnetic field allow for a detailed engineering of the surface states, including the possibility to carefully tune a gap in the Dirac cone at the surface.

First, let us develop our ideas within a simple generic band structure. We consider an effective low energy model near the Γ ($\mathbf{k} = 0$) point [3]. The four states near the Fermi energy at the Γ point are denoted using two quantum numbers, corresponding to spin $\sigma = \uparrow, \downarrow$ and parity $\tau = +, -$. Time reversal symmetry is represented by $\mathcal{T} = i\sigma_y\mathcal{K}$, where $\mathcal{K}$ is the complex conjugation operation. Inversion symmetry is represented using $\mathcal{I} = I \otimes \tau_z$. We study a Hamiltonian of the form

$$H = \vec{D}(\mathbf{k}) \cdot \vec{\gamma} \tag{1}$$

where $\vec{\gamma} = (\gamma_1, \gamma_2, \gamma_3; \gamma_5)$ are four Dirac matrices, which we represent by $\gamma_i = \sigma_i \otimes \tau_x$ with $i = 1, 2, 3$, $\gamma_5 = I \otimes \tau_z$. The remaining dirac matrices are defined as $\gamma_4 = I \otimes \tau_y$ and $\gamma_{ij} = -2i\,[\gamma_i, \gamma_j]$. In Eq. (1) and below, we denote 3-dimensional (space coordinate) vectors, such as the mo-

mentum, $\mathbf{k}$, in bold symbols, while the 4-dimensional vectors are denoted with a vector symbol $\vec{D}$, and $\hat{D}$ for unit vectors. Writing $\vec{D}(\mathbf{k}) = (\mathbf{d}(\mathbf{k}); D_5(\mathbf{k}))$, we note that the Hamiltonian (1) has both time reversal and space-inversion symmetries under the restriction that the vector $\mathbf{d}(\mathbf{k})$ be odd under inversion, while $D_5(\mathbf{k})$ is an even function.

Time-reversal-invariant ($\mathcal{T}^2 = -1$) band insulators in three dimensions admit a $\mathbb{Z}_2$ classification [14–16], falling into two categories - either topological, or trivial. The model in Eq. (1) can describe both phases, depending on the choice of parameters. Let us emphasize that while Eq. (1) does not describe the most general Hamiltonian with time reversal symmetry in three dimensions, this effective model does span a wide variety of realistic systems and allows for a relatively simple visualization of the $\mathbb{Z}_2$ topological invariant that we now focus on.

At each momentum, $\mathbf{k}$, the spectrum of the Hamiltonian (1) is doubly degenerate. Its eigenstates $\psi_{\mathbf{k}}$ of (1) are also the eigenstates of the rank-two projectors $P_{\pm}(\mathbf{k}) = \frac{1}{2}[I \pm \hat{D}(\mathbf{k}) \cdot \vec{\gamma}]$ onto the valence $(-)$ and conduction bands $(+)$. We can parameterize the unit vector, $\hat{D}(\mathbf{k}) = \vec{D}(\mathbf{k})/|\vec{D}(\mathbf{k})|$ (lying on a three-dimensional sphere, S^3), using two polar angles, θ and ξ, and an axial angle, ϕ. We define θ as $\cot(\theta_{\mathbf{k}}) = D_5(\mathbf{k})/|\mathbf{d}(\mathbf{k})|$. The angles ξ, ϕ correspond to the spin direction, by the unit vector $\hat{\mathbf{d}}(\xi_{\mathbf{k}}, \phi_{\mathbf{k}}) = \mathbf{d}(\mathbf{k})/|\mathbf{d}(\mathbf{k})|$. Note that there exists no global coordinate map on S^3 and in our case, $\hat{\mathbf{d}}(\xi_{\mathbf{k}}, \phi_{\mathbf{k}})$ remains undefined at $\theta = 0, \pi$.

Using the above parametrization, the topological invariant for Hamiltonians of the form (1) can be calculated by considering the map from the three dimensional Brillouin zone (BZ), which is a three dimensional torus, T^3, to S^3. The only topological invariant of this map is an integer which counts the number of times the map wraps the target space S^3, also called the degree of the map. Two Hamiltonians of the form (1), for which the degree of the map differs by 2, can be deformed into each other without closing the gap in the spectrum [17], by adding terms which digress from the form (1). Therefore, the $\mathbb{Z}_2$ classification of the insulator (1) is given by the degree of the map mod 2, with an even degree corresponding to a trivial insulator, and an odd degree to a topological one.

Near the Γ point, an expansion to order $\mathbf{k}^2$ yields

$$\vec{D}(\mathbf{k}) = (A\mathbf{k}; M - B\mathbf{k}^2), \tag{2}$$

where spherical symmetry can be assumed for convenience. The topological phase of the Hamiltonian (1),(2) occurs for $M/B > 0$. In this case, the angle, θ, changes from $\theta = 0$ at $\mathbf{k} = 0$ to $\theta = \pi$ at $|\mathbf{k}| \gg \sqrt{M/B}$. For each $0 < \theta < \pi$, the vector $\hat{\mathbf{d}}$ wraps a sphere of two dimensional unit vectors, S^2, which corresponds to a "latitude" on the target space S^3. Therefore, the target space S^3 of the map is covered once in the topological phase.

Consider now the case of $M/B < 0$. In this phase, the valence band is characterized by $0 \leq \theta < \pi/2$, while the conduction band corresponds to $\pi/2 > \theta \geq \pi$. Therefore, the degree of the map from the BZ to S^3 is zero, leading to a trivial insulator. We note that terms involving other γ matrices can be added to $H(\mathbf{k})$ in Eq. (1), while keeping time reversal symmetry. Then, the $\mathbb{Z}_2$ topological invariant cannot be calculated using the above simple considerations. However, as long as the added terms do not cause the gap in the spectrum of $H(\mathbf{k})$ to close, the $\mathbb{Z}_2$ invariant does not change.

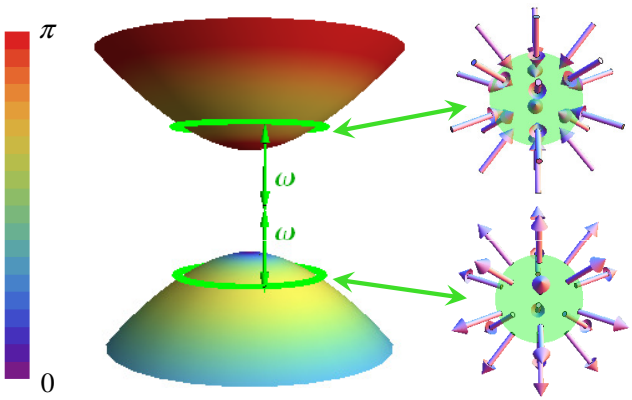

FIG. 1. The two paraboloids represent the dispersion relation $\epsilon_{\pm}(\mathbf{k})$ of the valence and conduction bands for the Hamiltonian (1) in the *trivial* phase, projected on $k_z = 0$. Each energy is doubly degenerate. At each momenta, the eigenstates of (1) can be represented by their direction in τ space, $tan(\theta) = |\langle\tau_x\rangle|/\langle\tau_z\rangle$, and spin direction $\hat{\mathbf{d}}(\xi, \phi) = (-1)^{\text{sign}\langle\tau_x\rangle}\langle\boldsymbol{\sigma}\rangle$. The color scheme of the paraboloids represents the value of the angle θ. The spin direction on spheres in momentum space, $|\mathbf{k}| = k_0$ is depicted on the right. A two photon resonance connecting the valence and conduction bands occurs at such a sphere in momentum space, and is represented by the green circles on the parabolas.

Having reviewed the construction of the $\mathbb{Z}_2$ topological index within the effective model (1), we now discuss a non-equilibrium case, where a time dependent perturbation is added to Eq. (1) initially in a trivial phase. As we shall see below, to induce a topological band structure in three dimensions using electromagnetic radiation, the external field has to satisfy non-trivial constraints. We first illustrate these requirements and elucidate the physics in the framework of the effective model with a generic time-dependent perturbation of the form:

$$V(t) = \text{Re}\left(\vec{V}e^{i\omega t}\right) \cdot \vec{\gamma} \tag{3}$$

where $\vec{V}$ is a complex, fixed, four-component vector. According to Floquet theory, the unitary operator describing the time-evolution of the system, $U(t) = \mathcal{P}\exp\left(-i\int_{t_0}^{t} dt H(t)\right)$, can be written as

$$U(t) = W(t)\exp\left[-iH_F(\mathbf{k})t\right] \tag{4}$$

where W is a unitary matrix satisfying $W(t+T) = W(t)$, $T = 2\pi/\omega$ and $H_F(\mathbf{k})$ is a time-independent Flo-

quet operator. The eigenstates of H_F are solutions of $[-i\partial_t + H(t)]\,\Psi = 0$ of the form $\Psi(t) = e^{-i\varepsilon t}\Phi(t)$, where $\Phi(t)$ is periodic with the period, T, and ε are called the quasi-energies. In the following, we shall take the time independent piece in the Hamiltonian, $H(\mathbf{k})$, to be in the trivial phase, and show that a topological spectrum for the Floquet operator $H_F(\mathbf{k})$ can be achieved nonetheless, by choosing $V(t)$ appropriately.

In three dimensions, and in the absence of particle-hole or sublattice symmetries, a topological spectrum requires time reversal symmetry [14–16]. The instantaneous Hamiltonian $H(\mathbf{k}, t) = H(\mathbf{k}) + V(t)$ does not necessarily posses such symmetry. However, if we can satisfy

$$\mathcal{T} H(\mathbf{k}, t)\mathcal{T}^{-1} = H(\mathbf{k}, -t + \tau) \tag{5}$$

for some fixed but arbitrary parameter, τ, then the Floquet operator $H_F(\mathbf{k})$ is invariant under an effective time reversal symmetry [7, 10]. The time-reversal constraint in Eq. (5) is satisfied if $\arg(V_{1,2,3}) = \arg(V_5) + \pi$.

The effect of the time-dependent potential becomes apparent in rotating frame, where the lower band is shifted up by ω. We transform the Hamiltonian to such a rotating frame via the unitary transformation $U(\mathbf{k}, t) = P_+(\mathbf{k}) + P_-(\mathbf{k})e^{-i\omega t}$ (here $P_\pm(\mathbf{k})$ are the projectors defined above). The resulting interaction-picture Hamiltonian reads

$$\begin{aligned} H_I(\mathbf{k}, t) = \epsilon_+(\mathbf{k})P_+(\mathbf{k}) + [\epsilon_-(\mathbf{k}) + \omega]\, P_-(\mathbf{k}) \\ + U(t)V(t)U^\dagger(t), \end{aligned} \tag{6}$$

where $\epsilon_\pm(\mathbf{k}) = \pm|\vec{D}(\mathbf{k})|$ are the band dispersion relations of $H(\mathbf{k})$. The Floquet operators corresponding to $H_I(t)$ and to $H(\mathbf{k})$ are *identical*, up to a (time-independent) unitary transformation.

Consider the first two terms in Eq. (6). In the interaction picture, the two bands intersect on a two-sphere in the BZ, $|\mathbf{k}| = k_0$, if the driving frequency ω is larger than the band gap, $2M$. We denote this two-sphere by $\mathcal{S}$, and we depict it in Fig 1. The driving term (third term in Eq. (6)) opens a gap in the quasi energy spectrum at $|\mathbf{k}| = k_0$. For momenta away from $\mathcal{S}$, the effect of the driving terms in Eq. (6) can be neglected [18], and the quasi-energy states are roughly eigenstates of $P_\pm(\mathbf{k})$. Notice, however, that the bands of H_I are inverted: the projector $P^I_-(\mathbf{k})$ onto the lower quasi-energy band of H_I, corresponds to $P_+(\mathbf{k})$ near the Γ point, and to $P_-(\mathbf{k})$ for $|\mathbf{k}| \gg k_0$ (and vice versa for $P^I_+(\mathbf{k})$). The projectors $P^I_\pm(\mathbf{k})$ smoothly interpolate between these two limits. In order to find the degree of the map from the BZ to S^3 that the projectors $P^I_\pm(\mathbf{k})$ define, we need to examine their properties on the resonance sphere $\mathcal{S}$.

For values of $\mathbf{k}$ near the resonance sphere, the rotating wave approximation (RWA) reveals the effect of the driving field. In this approximation, only time independent terms are kept in the last term of Eq. (6). This yields

$$V_{\mathrm{RWA}} = \tfrac{1}{2}\Big(P_+\check{V}P_- + P_-\check{V}^\dagger.P_+\Big), \qquad \check{V} = \vec{V}\cdot\vec{\gamma} \tag{7}$$

The topological properties of H_I are intimately related to the transformation properties of V_{RWA} under the group of spatial rotations in three dimensions. We shall take the action of this group in spin space to be $\exp(i\mathbf{m}\cdot\boldsymbol{\sigma})$, where $\mathbf{m}$ parameterizes the axis and angle of rotation. Note that while γ_5 transforms trivially under spatial rotations, $(\gamma_1, \gamma_2, \gamma_3)$ transform as a vector. Since to second order in $\mathbf{k}$ the projectors $P_\pm(\mathbf{k})$ are scalars, the transformation properties of V_{RWA} at this order are determined by those of $\check{V}$. Therefore, to second order in $\mathbf{k}$, V_{RWA} contains both scalar and vector representations of the rotation group. As we explain below, a scalar V_{RWA} yields $P^I_\pm(\mathbf{k})$ with a non-trivial topological $\mathbb{Z}_2$ invariant, as it maps the resonance sphere $\mathcal{S}$ to cover each spin direction once. However, a purely vector contribution to V_{RWA} yields a $P^I_\pm(\mathbf{k})$ which is topologically trivial, as the map from $\mathcal{S}$ covers only a partial cap of spin-directions.

The explicit form of V_{RWA} is

$$V_{\mathrm{RWA}} = \tfrac{1}{2}\Big(\vec{V_\perp}\cdot\vec{\gamma} + D_i \mathrm{Im}\{V_j\}\gamma_{ij}\Big) \tag{8}$$

where

$$\vec{V_\perp} = \mathrm{Re}\{\vec{V}\} - (\mathrm{Re}\{\vec{V}\}\cdot\hat{D})\hat{D}. \tag{9}$$

Two illuminating cases are: (i) $\vec{V} = V_5\hat{\mathbf{x}}_5$ and (ii) $\vec{V} = V_1\hat{\mathbf{x}}_1$, with V_1 and V_5 real. This gauge choice allows us, using Eq. (9), to approximate $P^I_\pm(\mathbf{k}) \approx \frac{1}{2}(1 \pm \hat{n}(\mathbf{k})\cdot\gamma)$, and study the map from the BZ to S^3 defined by $\hat{n}(\mathbf{k})$.

In case (i), $\check{V}$ is a scalar under spatial rotations, and hence so is $V_{\mathrm{RWA}} = \vec{V_\perp}\cdot\vec{\gamma}$. Therefore, the first three components of $\vec{V_\perp}$ must be proportional to $\mathbf{k}$ while the fifth components is a scalar. Indeed, using Eq. (9) we get

$$\vec{V_\perp} = \Big(-\frac{V_5 D_5}{D^2}A\mathbf{k}, V_5 - \frac{V_5 D_5^2}{D^2}\Big) \tag{10}$$

where $D = |\vec{D}(\mathbf{k})|$. On the resonance sphere $\mathcal{S}$, we have $\hat{n}(\mathbf{k}, t)\Big|_{\mathcal{S}} = \vec{V_\perp}/|\vec{V_\perp}|$, which maps $\mathcal{S}$ to an S^2 sphere with fixed latitude $\theta(k_0)$ in the target space S^3. Therefore, $\hat{n}(\mathbf{k})$ defines a map from the BZ to S^3, which maps the Γ point to the *south* pole, S^2 spheres in the BZ to S^2 spheres ("latitudes") on S^3, and maps $\mathbf{k} \gg k_0$ towards the *north* pole of S^3. It is therefore a map of degree one, which implies a topological spectrum.

In Case (ii), however, $\check{V}$ and V_{RWA} give a vector representation of spatial rotations. Therefore, the first three components of $\vec{V_\perp}$ must either be scalars or belong to a spin-2 representation of spatial rotations, while the fourth and fifth components must belong to a vector representation. Indeed, an explicit calculation gives

$$\vec{V_\perp} = \Big(V_1\hat{\mathbf{x}} - V_1\frac{A^2 k_x \mathbf{k}}{D^2}, V_1\frac{Ak_x}{D}\frac{D_5}{D}\Big) \tag{11}$$

Clearly, on $\mathcal{S}$, the vector $\vec{V_\perp}$ does not wrap around an S^2 sphere on S^3, and the resulting map defined by $\hat{n}(\mathbf{k})$ is topologically trivial.

More generally, $V_{\rm RWA}$ will be a superposition of a scalar and vector component. Whether a topological spectrum is obtained depends on the relative magnitude of the two components.

Let us now apply the geometrical considerations leading to a topological Floquet spectrum in 3D, to oscillating electromagnetic fields. The electric field operator is a vector under spatial rotations. Therefore, in light of the above discussion, it first seems impossible that it could induce a topological Floquet spectrum. This can be remedied by considering multipole tensors of the electric field. The quadrupole tensor E_iE_j can be decomposed into a scalar, which is given by its trace, and a tensor giving a spin-2 representation of spatial rotations. In the following, we show how to use the scalar part of the quadrupole tensor in order to induce a topological Floquet spectrum. The scheme involves choosing a frequency ω which satisfies $M/2 < \omega < M$. Such a choice for the frequency precludes a resonance induced by a single-photon transition, which is linear in the driving electric field $\mathbf{E}$, but allows for a two-photon transition, which is second order in $\mathbf{E}$, and therefore involves the quadrupole tensor.

Note that in order to satisfy the time reversal symmetry constraint, as defined by Eq. (5), the oscillating field must be *linearly* polarized [10]. An ellipticity in the polarization of the driving field leads to interesting effects, which will be discussed later. We choose a gauge $\mathbf{E} = \partial_t \mathbf{A}$, $\phi = 0$, whereby the Hamiltonian becomes $H = \vec{D}(\mathbf{k} + \mathbf{A}(t)) \cdot \vec{\gamma}$. Choosing $\mathbf{A} = \mathcal{A}_0 \cos(\omega t)\hat{\mathbf{x}}$, we obtain the Hamiltonian

$$H(t) = \vec{D}'(\mathbf{k}) \cdot \vec{\gamma} + \vec{V}_1 \cdot \vec{\gamma} \cos(\omega t) + \vec{V}_2 \cdot \vec{\gamma} \cos(2\omega t), \quad (12)$$

with $\vec{V}_1 = A\mathcal{A}_0 \hat{\mathbf{x}} - 2B\mathcal{A}_0 k_x \hat{\mathbf{x}}_5$, $\vec{V}_2 = -\frac{1}{2} B\mathcal{A}_0^2 \hat{\mathbf{x}}_5$, and $\vec{D}'(\mathbf{k}) = \Big(A\mathbf{k}; M - B\mathcal{A}_0^2 - B\mathbf{k}^2\Big)$. Below we sketch the outline of the calculation, the details of which are given in Appendixes A and B.

The two-photon resonance is a second order process in the electric field. In the chosen gauge, a 2ω-term arises both directly from $\vec{V}_2$, and from a second order process in $\vec{V}_1$. The contribution of both terms to $V_{\rm RWA}$ scales, to lowest order in the light intensity, as $\mathcal{A}_0^2/M$. In order to calculate their effect, we perform two consecutive unitary transformations (see Appendix B for an alternative derivation). We first perform a transformation to a frame rotating with frequency ω, of the form leading to Eq. (6). The resulting interaction picture Hamiltonian does not contain any resonances. We diagonalize its time independent terms, which yields new eigenvalues and projection operators, which we denote by $\varepsilon_{\pm}^{(1)}(\mathbf{k})$ and $P_{\pm}^{(1)}(\mathbf{k})$ respectively. A second unitary transformation, $U_2(\mathbf{k}, t) = P_+^{(1)} + P_-^{(1)} \exp(-i\omega t)$ yields a new interaction picture Hamiltonian

$$H_2 = \varepsilon_+^{(1)}(\mathbf{k}) P_+^{(1)} + (\varepsilon_-^{(1)}(\mathbf{k}) + \omega) P_-^{(1)} + U_2 \mathcal{V}^{(1)}(t) U_2^\dagger \quad (13)$$

where $\mathcal{V}^{(1)}(t)$ denotes the time dependent terms resulting from the first transformation.

After the second transformations, the two bands cross at a surface $\mathcal{S}$ with $\varepsilon_+^{(1)}(\mathbf{k}) = (\varepsilon_-^{(1)}(\mathbf{k}) + \omega)$ and the topology of a sphere. We now employ the rotating wave approximation, which yields on the resonance surface,

$$H_{2,\rm RWA}|_{\mathcal{S}} = \tfrac{1}{2} \vec{V}_\perp^{(1)} \cdot \vec{\gamma}. \quad (14)$$

The vector $\vec{V}_\perp^{(1)}$ is defined, to lowest order in $\mathcal{A}_0$ and $\mathbf{k}$, as in Eq. (9) with the replacement $\hat{D} \to \hat{D}^{(1)}$ and $\vec{V} \to \vec{V}^{(1)} \equiv \Big((\vec{V}_1 - \vec{V}_2) \cdot \hat{D}\Big) \hat{D} + \vec{V}_2$ (see Appendix A for details). The contribution to $\vec{V}_\perp^{(1)}$ which allows for a topological map comes from the term corresponding to $\vec{V}_2$ in Eq. (12). A quick inspection shows that $\vec{V}_2 \cdot \vec{\gamma}$ is a scalar under spatial rotation, and after the two transformations yields a contribution to $\vec{V}_\perp^{(1)}$ of the form appearing in Eq. (10), with corrections to its spatial components of higher order in $\mathbf{k}$ and $\mathcal{A}_0$. The contribution to $\vec{V}_\perp^{(1)}$ coming from $\vec{V}_1$ in Eq. (12) only leads to an anisotropy of the gap in the Floquet spectrum, and does not change the topological properties of $\vec{V}_\perp^{(1)}$ on the resonance sphere $\mathcal{S}$.

The first three components of the vector field $\vec{V}_\perp^{(1)}$ are plotted in Fig. 2. Clearly, they map $\mathcal{S}$ to a single covering of the unit sphere. Note that the 5^{th} component of $\vec{V}_\perp^{(1)}$ is not constant on $\mathcal{S}$. This does not change the degree of the map from the BZ to S^3, and the Floquet spectrum is characterized by a non-trivial $\mathbb{Z}_2$ invariant. The magnitude of the gap on the resonance surface is not isotropic. This is expected, as choosing the polarization direction breaks the rotational symmetry of the problem. On the resonance, the Floquet spectrum is fully gapped, where the smallest gap occurs for $k_x = 0$, and is given by

$$E_{\rm gap} = \frac{AB\mathcal{A}_0^2}{4M} |\mathbf{k}_{\mathcal{S}}| \quad (15)$$

where $\mathbf{k}_{\mathcal{S}}$ is the resonance wave vector.

One of the most striking consequences of the topological band structure in three dimensions are the mid-gap surface modes , which are characterized by a single Dirac cone [19]. Likewise, a striking consequence of the above considerations are the appearance of surface modes in the presence of the driving electric field. The surface quasi-energy states appear inside the Floquet quasi-energy gap and are characterized by a single Dirac cone.

To demonstrate this, we use exact numerical methods to study the Floquet problem of a tight binding model corresponding to the Hamiltonian of Eq. (1). We consider a finite slab with vanishing boundary conditions at $z = 0, L$ and a driving electric field polarized in the $\hat{\mathbf{x}}$ direction. The quasi energy and momenta in the $\hat{\mathbf{x}}$ and $\hat{\mathbf{y}}$ directions are good quantum numbers. In Fig. 3, we plot the quasi energy spectrum inside the quasi-energy gap, which clearly exhibits a single dirac cone. Note that the Dirac cone is not isotropic, resulting from the choice of the polarization along the $\hat{\mathbf{x}}$ direction.

Broken time reversal symmetry on the surface of a three dimensional topological insulator leads to a gap at

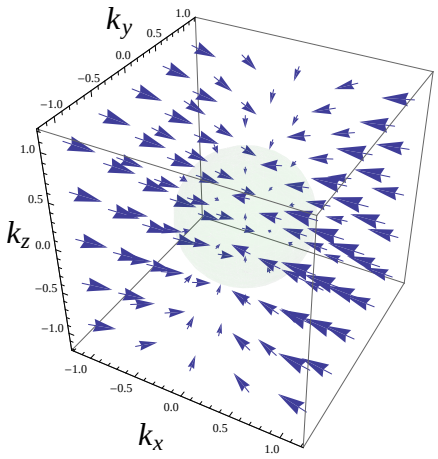

FIG. 2. The first three components of the vector field $\vec{V}_{\perp}^{(1)}(\mathbf{k})$ resulting from a two photon resonance of a linearly polarized electro-magnetic field. The magnitude of the plotted vector field, on the resonance sphere $\mathcal{S}$ (depicted), gives the gap in the Floquet spectrum. Its direction determines the spin direction of the quasi-energy states on $\mathcal{S}$. The map from $\mathcal{S}$ to the two-sphere S^2, defined by these three components, is of degree one. The resulting gap in the Floquet spectrum is not isotropic, due to the necessary choice of the direction of polarization of the electric field.

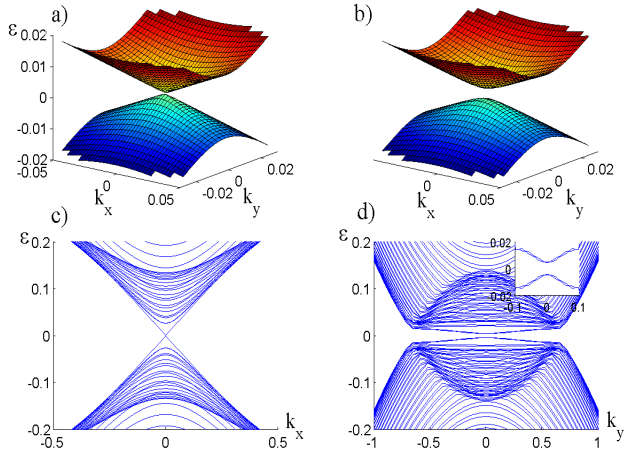

FIG. 3. Quasi-energy spectrum of the Floquet operator corresponding to Eq. (12), in the slab geometry: periodic boundary conditions in the x, y directions and vanishing ones in the z direction. In a) and b), we plot the quasi-energy spectrum inside the gap of the Floquet spectrum, as a function k_x, k_y, for different polarizations of the driving field. a) Linearly polarized electric field, $\boldsymbol{\varepsilon} = \hat{\mathbf{x}}$, yielding a Dirac cone on the surface. b) A small gap in the surface spectrum is opened for an elliptical polarization with small ellipticity, $\boldsymbol{\varepsilon} = \hat{\mathbf{x}} + i\delta\hat{\mathbf{y}}$, with $\delta = 0.05$. Note that in both a) and b), the Dirac cone is not isotropic. c), d) Quasi-energy spectrum, showing bulk bands and edge states. c) Spectrum as function of k_x, for $k_y = 0$, with $\boldsymbol{\varepsilon} = \hat{\mathbf{x}}$. d) Quasi-energy spectrum as a function of k_y, for $k_x = 0$, $\boldsymbol{\varepsilon} = \hat{\mathbf{x}} + i\delta\hat{\mathbf{y}}$. The inset magnifies the gapped Dirac surface spectrum. Note that the the gap in the Floquet spectrum is enhanced for $k_x > 0$, as evident by comparing the spectra in c) and d)

the Dirac node of the surface states. Such a gap entails unique consequences in terms of transport properties of the surface states, as it leads to a half integer quantum hall effect on the surface. Remarkably, a gap at the Dirac node of the surface Floquet spectrum can be easily controlled by an appropriate tuning of the polarization of the electromagnetic driving field. Consider an elliptically polarized electric field, $\mathbf{E} = \mathrm{Re}\mathbf{E}e^{i\omega t}$ with $\boldsymbol{\varepsilon} = \mathbf{E}/|\mathbf{E}| = (\hat{\mathbf{x}} + i\delta\hat{\mathbf{y}})$. The electric field operator is even under time reversal. Therefore Eq. (5) cannot be satisfied for any $\delta \neq 0$. The gap in the Dirac cone on the surface depends quadratically on the elipticity parameter δ.

The analysis above demonstrates how to obtain a "time reversal" invariant topological spectrum in three dimensions, by periodically driving a topologically trivial system. Our approach could be applied in a variety of quantum systems, e.g., cold atoms with synthetic spin orbit couplings [20, 21]. The most natural experimental application of our results are in semiconductors with appropriate properties, namely, a spectrum with a narrow direct band-gap occurring in one (or an odd number) of points in the Brillioun zone. Candidate materials are Sb_2Se_3 in the rhombohedral crystal structure [3], $GeSb_2Te_4$ [22]. Moreover, Heusler compounds [23, 24] with applied strain exhibit four bands and a narrow bandgap near the Γ point, and are therefore excellent candidates for our proposal. In the materials mentioned above, a sizable gap in the Floquet spectrum, on the order of $10K$, can be achieved using electric fields of $10^4 V/m$.

The surface modes in the Floquet spectrum predicted in this work could be directly probed using photoemission spectroscopy [25, 26]. Moreover, a gapped surface Floquet spectrum can be detected using the Kerr and Faraday effect [27], whereas in the material these effects should be negligible absent the driving. The emergent Floquet spectrum discussed above is that of a band inverted semiconductor [28], and in any steady state we can expect a finite density of particles and holes in the Floquet bands [29],[30]. One concern is that these free charge carriers may attenuate the driving electromagnetic field. For a lower bound of the attenuation length ζ we assume that all electrons participating in the band inversion act as free charge carriers. This leads to $\zeta \sim \sqrt{\rho} \sim 1/\sqrt{\mu n}$, with carrier density $n \sim k_0^3$ and mobility μ. Since the localization length λ of the surface modes scales linearly with k_0^{-1}, a parameter regime in which $\lambda < \xi$ could be found, according to material parameters.

Acknowledgements: We thank Joseph Avron, Erez Berg, Daniel Podolsky, and John Preskill for helpful discussions. VG was supported by NSF CAREER award. NL was supported by the Gordon and Betty Moore Foun-

dation and NSF through Caltech's Institute of Quantum Information and Matter, and by the National Science Foundation under Grant No. PHY-0803371. DLB was supported by the Sherman Fairchild foundation. GR and VG acknowledge support from DARPA. We are also grateful for the hospitality of the Aspen Physics Center where part of this work was done. We also acknowledge hospitality of the KITP and the National Science Foundation under Grant No. NSF PHY05-51164.

Appendix A: Topological properties of the two-photon resonance

In this section we study the topological properties of the Floquet operator corresponding to an insulator driven with an electromagnetic field whose frequency allows only for a two photon resonance, $M < \omega < 2M$, where $2M$ is the bandgap of the insulator. The two-photon resonance is a second order process in the electric field. In the chosen gauge, a 2ω-term arises both directly from $\vec{V}_2$, and from a second order process in $\vec{V}_1$. Both terms therefore yield contributions of order $\mathcal{A}_0^2$. In order to consider both terms on an equal footing we shall perform two consecutive time dependent unitary transformations, where each transformation is characterized by the frequency ω. In order to analyze the resulting time dependent Hamiltonian, we shall employ the rotating wave approximation and expand to lowest orders in $\mathbf{k}$ and $\mathcal{A}_0$.

We first introduce some useful notations. We decompose any four dimensional vector $\vec{V}$ into the components parallel and perpendicular to a four dimensional unit vector $\hat{D}$ as

$$\vec{V}_{\perp\hat{D}} = \vec{V} - \left(\vec{V}\cdot\hat{D}\right)\hat{D}, \tag{A1}$$

and

$$\vec{V}_{\parallel\hat{D}} = \left(\vec{V}\cdot\hat{D}\right)\hat{D}. \tag{A2}$$

For notational convenience, we shall relabel $\vec{D}'(\mathbf{k}) \to \vec{D}(\mathbf{k})$, c.f. Eq. (12). The first rotating wave transformation is done via the unitary

$$U_1(\mathbf{k},t) = P_+(\mathbf{k}) + P_-(\mathbf{k})e^{-i\omega t}, \tag{A3}$$

which leads to the Hamiltonian in the first rotating frame given by

$$\begin{aligned} H_1 &= U_1(\mathbf{k},t)H(t)U_1^\dagger(\mathbf{k},t) \\ &= \left(\vec{D}(\mathbf{k}) + \tfrac{1}{2}\vec{V}_{1\perp\hat{D}}\right)\cdot\vec{\gamma} + \omega P_-(\mathbf{k}) + \mathcal{V}^{(1)}(t). \end{aligned} \tag{A4}$$

In the above, the time dependent part is given by

$$\begin{aligned} \mathcal{V}^{(1)}(t) = \quad & (\vec{V}_{1\parallel\hat{D}} + \tfrac{1}{2}\vec{V}_{2\perp\hat{D}})\cdot\vec{\gamma}\cos(\omega t) \\ & + \tfrac{1}{2}(\vec{V}_{2\perp\hat{D}})_i\hat{D}_j\gamma_{ij}\sin(\omega t) + \tilde{\mathcal{V}}(t). \end{aligned} \tag{A5}$$

Note that $\mathcal{V}^{(1)}(t)$ contains terms with frequencies ω (the first two term in Eq. (A5)) and $2\omega, 3\omega$ (corresponding to $\tilde{\mathcal{V}}(t)$, the third term above).

It is convenient to define

$$\hat{D}^{(1)}(\mathbf{k}) = \Delta\epsilon(\mathbf{k})\hat{D}(\mathbf{k}) + \tfrac{1}{2}\vec{V}_{1\perp\hat{D}}(\mathbf{k}), \tag{A6}$$

with

$$\Delta\epsilon(\mathbf{k}) = \epsilon(\mathbf{k}) - \tfrac{1}{2}\omega, \qquad \epsilon(\mathbf{k}) = |\bar{D}(\mathbf{k})|, \tag{A7}$$

which enables us to write Eq. (A4) as

$$H_1 = \hat{D}^{(1)}(\mathbf{k})\cdot\vec{\gamma} + \mathcal{V}^{(1)}(t) \tag{A8}$$

The time-independent part of Eq. (A4) can be expressed using eigenvalues $\varepsilon_\pm^{(1)}(\mathbf{k})$ and projection operators $P_\pm^{(1)}(\mathbf{k})$. We now perform a second rotating wave transformation

$$U_2(\mathbf{k},t) = P_+^{(1)}(\mathbf{k}) + P_-^{(1)}(\mathbf{k})\exp(-i\omega t), \tag{A9}$$

which yields the Hamiltonian in the 2^{nd} frame,

$$\begin{aligned} H_2 = {} & \varepsilon_+^{(1)}(\mathbf{k})P_+^{(1)}(\mathbf{k}) + (\varepsilon_-^{(1)}(\mathbf{k}) + \omega)P_-^{(1)}(\mathbf{k}) \\ & + U_2(\mathbf{k},t)\Big((\vec{V}_{1\parallel\hat{D}} + \tfrac{1}{2}\vec{V}_{2\perp\hat{D}})\cdot\vec{\gamma}\Big)U_2^\dagger(\mathbf{k},t)\cos(\omega t) \\ & + U_2(\mathbf{k},t)\Big((\tfrac{1}{2}\vec{V}_{2\perp\hat{D}})_i\hat{D}_j\gamma_{ij}\Big)U_2^\dagger(\mathbf{k},t)\sin(\omega t). \end{aligned} \tag{A10}$$

In the above, we have omitted from H_2 the term $U_2\tilde{\mathcal{V}}(t)U_2^\dagger$ which does not contain any time independent contributions to H_2, and therefore does not contribute to the two photon resonance.

After the second transformations, the two bands cross at a surface $\mathcal{S}$ for which $\varepsilon_+^{(1)}(\mathbf{k}) = (\varepsilon_-^{(1)}(\mathbf{k}) + \omega)$. We now employ the rotating wave approximation. The contribution coming from the second term in Eq. (A10) can be deduced from inspecting Eq. (8) and (9) in the main text. The contribution arising from the third term in Eq. (A10) yields a term of the form $\frac{1}{4i}\hat{D}_i(\vec{V}_{2\perp\hat{D}})_j\hat{D}_k[\gamma_{ij},\gamma_k]$. Some algebra reveals that to lowest order in $\mathcal{A}_0$ and $\mathbf{k}$, the two terms in Eq. (A10) involving $\vec{V}_{2\perp\hat{D}}$ yield the same contribution to the rotating wave approximation.

Therefore, on the surface $\mathcal{S}$ we have,

$$H_{2,\text{RWA}}|_{\mathcal{S}} = \frac{1}{2}\vec{V}^{(1)}_{\perp\hat{D}^{(1)}}\cdot\vec{\gamma} \tag{A11}$$

where the vector $\vec{V}^{(1)}_{\perp\hat{D}^{(1)}}$ is defined as in Eq. (A1) by replacing

$$\hat{D} \to \hat{D}^{(1)}, \qquad \vec{V} \to \vec{V}^{(1)} = \vec{V}_{1\parallel\hat{D}} + \vec{V}_{2\perp\hat{D}}. \tag{A12}$$

In order to achieve a topological Floquet spectrum, the vector field $\vec{V}^{(1)}_{\perp\hat{D}^{(1)}}$ needs to map the resonance surface $\mathcal{S}$ to an S^2 sphere on the three dimensional sphere S^3. In the following we shall show that this is indeed the case.

As a first step, we inspect the contributions to $\vec{V}^{(1)}$, which arise after the first unitary transformation. Keeping only terms only up to second order in $\mathbf{k}$, we find

$$\vec{V}_{1\|\hat{D}} = \frac{\mathcal{A}_0(A^2-2BM)}{M} k_x \Big(\frac{A}{M}\mathbf{k}, 1\Big),$$

and

$$\vec{V}_{2\perp\hat{D}} = \frac{AB\mathcal{A}_0^2}{2M}\left(\mathbf{k}, -\frac{A}{M}\mathbf{k}^2\right). \tag{A13}$$

The vector field $\vec{V}_{2\perp}$ clearly maps a sphere in the BZ to an S^2 sphere on the target space S^3. This is of course expected from noting that $\vec{V}_2\cdot\vec{\gamma}$ is a scalar under spatial rotations. However, we are interested in its contribution to the two-photon resonance, *i.e.*, to Eq. (A11).

To this end, we note that $\vec{V}_{2\perp\hat{D}}$ is orthogonal to $\hat{D}$ by construction, and $\hat{D}^{(1)} = \hat{D} + o\Big(\frac{|\vec{V}_{1\perp}|}{\Delta\epsilon}\Big) \approx \hat{D} + o\Big(\frac{|\mathcal{A}_0|}{M}\Big)$. Therefore, the correction to $\vec{V}_{2\perp\hat{D}}$, when it is inserted into the expression for $\vec{V}^{(1)}_{\perp\hat{D}^{(1)}}$, are of higher order in $\mathcal{A}_0$. Explicitly, we have

$$\begin{aligned}\vec{V}_{2\perp\hat{D}}\cdot\hat{D}^{(1)} &= \frac{1}{2|\vec{D}^{(1)}|}\vec{V}_{2\perp}\cdot\vec{V}_1 \\ &= \frac{1}{|\vec{D}^{(1)}|}\frac{AB\mathcal{A}_0^3}{4M}\Big(A + 2\frac{AB}{M}\mathbf{k}^2\Big)k_x \\ &\approx \frac{1}{\Delta\epsilon(\mathbf{k})}\frac{A^2B\mathcal{A}_0^3}{4M}k_x\end{aligned}$$

where we have kept terms only up to order $\mathbf{k}^2$ and $\mathcal{A}_0^3$. Therefore, the final contribution of $\vec{V}_2$ to $\vec{V}^{(1)}_{\perp\hat{D}^{(1)}}$ to this order is

$$\vec{V}_{2\perp\hat{D}^{(1)}} = \vec{V}_{2\perp\hat{D}} - \Big(\frac{A^2B\mathcal{A}_0^3}{4M\Delta\epsilon(\mathbf{k})}k_x\Big)\hat{D} \tag{A14}$$

The second term in the above equation correspond to a correction to the spatial $(1-3)$ parts of $\vec{V}_{2\perp\hat{D}}$, Eq. (A13), of order $\mathbf{k}^2$ and $\mathcal{A}_0^3$. The spatial part of $\vec{V}_{2\perp\hat{D}}$ are originally of order $\mathbf{k}$ and $\mathcal{A}_0^2$. Therefore, to lowest order in $\mathbf{k}$ and $\mathcal{A}_0$, this correction does not alter the topological property of $\vec{V}^{(1)}_{\perp\hat{D}^{(1)}}$, which we shall describe below.

We now calculate the contribution of $\vec{V}_1$ to $\vec{V}^{(1)}_{\perp\hat{D}^{(1)}}$, which will turn out to be of the same order as the contribution of $\vec{V}_2$, c.f. Eq. (A14).

First, we note that

$$\vec{V}_{1\|\hat{D}}\cdot\hat{D}^{(1)} = \frac{\Delta\epsilon}{|\vec{D}^{(1)}|}\Big(\vec{V}_1\cdot\hat{D}\Big) \tag{A15}$$

From Eq. (A15), and for $\Delta\epsilon(\mathbf{k}) \gg |\vec{V}_{1\perp\hat{D}}|$, we have

$$\begin{aligned}\big(\vec{V}_{1\|\hat{D}}\cdot\hat{D}^{(1)}\big)\hat{D}^{(1)} &= \big(1 - \frac{|\vec{V}_{1\perp\hat{D}}|^2}{8\Delta\epsilon^2}\big)\Big(\vec{V}_1\cdot\hat{D}\Big) \\ &\times \big(1 - \frac{|\vec{V}_{1\perp\hat{D}}|^2}{8\Delta\epsilon^2}\big)\big(\hat{D} + \frac{\vec{V}_{1\perp\hat{D}}}{2\Delta\epsilon}\big)\end{aligned} \tag{A16}$$

Using the definition of $\vec{V}_{1\|}$, Eq. (A2), we see that the total contribution of $\vec{V}_1$ to $\vec{V}^{(1)}_{\perp\hat{D}^{(1)}}$, to order $\mathcal{A}_0^2$ is

$$\vec{V}_{1\|} - \big(\vec{V}_{1\|}\cdot\hat{D}^{(1)}\big)\hat{D}^{(1)} \approx -\frac{\Big(\vec{V}_1\cdot\hat{D}\Big)}{2\Delta\epsilon}\vec{V}_{1\perp} \tag{A17}$$

Therefore, this contribution to $\vec{V}^{(1)}_{\perp\hat{D}^{(1)}}$ is of the *same* order in the driving field as the contribution coming from $\vec{V}_{2\perp\hat{D}}$, Eq. (A13) and its inclusion was necessary for completeness. Note that $\vec{V}_{1\perp} = A\mathcal{A}_0\hat{\mathbf{x}} + o(|\mathbf{k}|)$, and therefore

$$\frac{\Big(\vec{V}_1\cdot\hat{D}\Big)}{2\Delta\epsilon}\vec{V}_{1\perp\hat{D}}\cdot\hat{\mathbf{x}} = \frac{\mathcal{A}_0^2\big(A^2-2BM\big)}{2M\Delta\epsilon}Ak_x + o(\mathcal{A}_0^2, |\mathbf{k}|^3) \tag{A18}$$

while the y and z components of Eq. (A17) are of order $\mathcal{A}_0^2$ and $\mathbf{k}^3$. Note that the $\hat{x}_5$ component of Eq. (A17) is of order $\mathcal{A}_0^2$ and $\mathbf{k}^2$. From Eq. (A16), we see that the $\vec{V}_1$ term also contributes terms of order $\mathcal{A}_0^3$ and $\mathbf{k}^2$ to $\vec{V}^{(1)}_{\perp\hat{D}^{(1)}}$. All of the above higher order corrections do not change the topological properties of $\vec{V}^{(1)}_{\perp\hat{D}^{(1)}}$, to lowest order in $\mathcal{A}_0$ and $\mathbf{k}$.

Summing up both contributions to $\vec{V}^{(1)}_{\perp\hat{D}^{(1)}}$, we have, to lowest order in $\mathbf{k}$ and $\mathcal{A}_0$,

$$\begin{aligned}\vec{V}^{(1)}_{\perp\hat{D}^{(1)}}\cdot\hat{\mathbf{x}} &= \Big(\vec{V}_{2\perp\hat{D}} - \frac{\Big(\vec{V}_1\cdot\hat{D}\Big)}{2\Delta\epsilon}\vec{V}_{1\perp}\Big)\cdot\hat{\mathbf{x}} \\ &= \frac{\mathcal{A}_0^2}{2M}\Big(B - (A^2-2BM)/\Delta\epsilon\Big)Ak_x,\end{aligned} \tag{A19}$$

while the other two spatial components are given by

$$\vec{V}^{(1)}_{\perp\hat{D}^{(1)}}\cdot\hat{\mathbf{x}}_\alpha = \frac{\mathcal{A}_0^2B}{2M}Ak_\alpha, \qquad \alpha = y, z \tag{A20}$$

From Eqs. (A19,A20), we see that the vector field $\vec{V}^{(1)}_{\perp\hat{D}^{(1)}}$ maps the resonance surface $\mathcal{S}$ to an 2-sphere on the target space S^3. This 2-sphere is not at a constant "latitude", *i.e.* its θ coordinate on S^3 is not constant. Importantly however, this 2-sphere winds around the poles of S^3, *i.e.*, it is an incontractible sphere on the space $S^3\setminus(N\cup S)$, the space of S^3 with the north and south pole removed.

From the above considerations, we see that $H_2(t)$, given in Eq. (A10) can be characterized by projection operators of the form $P^{(2)}_\pm(\mathbf{k}) = \frac{1}{2}(1 \pm \hat{n}_2(\mathbf{k})\cdot\vec{\gamma})$. The unit vector $\hat{n}_2(\mathbf{k})$ defines a map from the BZ to S^3 with the properties: (i) For regions in the BZ near the Γ point, $\hat{n}_2(\mathbf{k}) \approx -\hat{D}(\mathbf{k})$, and therefore it maps 2-spheres in the BZ to 2-spheres on S^3, close to its *south* pole; (ii) Maps the sphere $\mathcal{S}$ in the BZ to an S^2 sphere on S^3 which is incontractible on $S^3\setminus(N\cup S)$ (as discussed above) ; (iii) For large values of $\mathbf{k}$, $\hat{n}(\mathbf{k}) \approx \hat{D}(\mathbf{k})$, therefore these are mapped to 2-spheres close to the *north* pole of S^3. From continuity of $\hat{n}_2(\mathbf{k})$, it must therefore define a map of degree one. This implies that the Floquet operator corresponding to $H_2(t)$ and $H(t)$, has a non trivial $\mathbb{Z}_2$ topological invariant.

Appendix B: Virtual absorption perturbation theory

The two consecutive RW transformations are very reminiscent of a perturbation expansion. One RW transformation fails to produce a degenracy, and therefore a second transformation is necessary to expose the role of two-photon processes. In this section we will show how indeed such processes can be analyzed as virtual absorption processes, and derive a formula which replaces second-order degenerate perturbation expansions.

The first step involves mapping the time-dependent Floquet problem to a time-independent problem using an auxiliery degree of freedom. Let us introduce an additional Hilbert space which serves as a counter of photons absorbed (for the experts, we note that this auxiliery variable is just a way of keeping track of the Floquet block index). We introduce an infinite lattice for a single particle, which we denote F, with states $|n\rangle_F$; n is essentially counting the number of photons absorbed by the system. The original system has a Hamiltonian which is split to time independent $\mathcal{H}_{sys}$ and time dependent pieces:

$$H(t) = H_{sys} + \hat{O}e^{i\omega t} + \hat{O}^\dagger e^{-i\omega t}, \tag{B1}$$

we now replace the time dependent terms with hopping terms for the register particle F. We also add a diagonal energy term that determines the energy of the F states. The Hilbert space after this mapping is a tensor product state between the F-states and the system's states. The time dependent Hamiltonian is therefore replaced by an operator that acts on the larger Hilbert space,

$$\mathcal{H}_F = \mathcal{H}_{sys} + \sum_n \left(\hat{O} \left|n+1\right\rangle_{F\ F} \left\langle n\right| + \hat{O}^\dagger \left|n\right\rangle_{F\ F} \left\langle n+1\right| \right) + \mathcal{H}_\omega, \tag{B2}$$

with

$$\mathcal{H}_\omega = \sum_n n\omega \left|n\right\rangle_{F\ F} \left\langle n\right|. \tag{B3}$$

and $\mathcal{H}_{sys} = H_{sys} \otimes \mathbb{I}_F$.

To retrieve the original Hamiltonian, Eq. (B1) all that is necessary is to initiate the auxiliary F-states in the zero-momentum state:

$$\left|\psi\right\rangle_F = \frac{1}{N} \sum_n \left|n\right\rangle_F. \tag{B4}$$

with N providing a normalization.

Our first claim is that the time-independent Hamiltonian, Eq. (B2), initiated with $\left|\psi\right\rangle_F$ has the same propagator for the system as the one for the original Hamiltonian, Eq. (B1):

$$U(t) = \mathcal{P}\left[\exp\left[-i\int_0^t dt H(t)\right]\right] =_F \left\langle\psi\right| \exp[i\mathcal{H}_\omega t] \exp\left[-i\mathcal{H}_F t\right] \left|\psi\right\rangle_F. \tag{B5}$$

where $\mathcal{P}$ denotes path ordering. To show this, we first move to the interaction picture in terms of the states F. More precisely we consider:

$$\mathcal{U}(t) = e^{i\mathcal{H}_\omega t} \cdot e^{-i\mathcal{H}_F t}. \tag{B6}$$

We note that

$$\frac{d\mathcal{U}(t)}{dt} = -ie^{i\mathcal{H}_\omega t}(\mathcal{H}_F - \mathcal{H}_\omega)e^{-i\mathcal{H}_\omega t}\mathcal{U}(t). \tag{B7}$$

Since $\mathcal{H}_F - \mathcal{H}_\omega = \mathcal{H}_{sys} + \mathcal{H}_{OF}$, we write:

$$e^{i\mathcal{H}_\omega t}(\mathcal{H}_F - \mathcal{H}_\omega)e^{-i\mathcal{H}_\omega t} = \mathcal{H}_{sys} + \mathcal{H}_{OF}(t) \tag{B8}$$

with:

$$\mathcal{H}_{OF}(t) = e^{i\mathcal{H}_\omega t} \sum_n \left(\hat{O} \left|n+1\right\rangle_{F\ F} \left\langle n\right| + \hat{O}^\dagger \left|n\right\rangle_{F\ F} \left\langle n+1\right| \right) e^{-i\mathcal{H}_\omega t} = \sum_n \left(\hat{O} \left|n+1\right\rangle_F\ _F \left\langle n\right| e^{i\omega t} + \hat{O}^\dagger \left|n\right\rangle_{F\ F} \left\langle n+1\right| e^{-i\omega t} \right). \tag{B9}$$

$\mathcal{U}(t)$ is easily solved to be:

$$\mathcal{U}(t) = \mathcal{P}\left[\exp\left[-i\int_0^t dt\left(\mathcal{H}_{sys} + \mathcal{H}_{OF}(t)\right)\right]\right] \tag{B10}$$

And therefore, the identity (B5), which we are trying to prove, becomes

$$U(t) =_F \langle\psi|\mathcal{U}(t)\,|\psi\rangle_F\,. \tag{B11}$$

Now that we have essentially eliminated $\mathcal{H}_\omega$ from the expression for $U(t)$, the only operators relating to the F-states remaining are the hopping operators $\sum_n |n+1\rangle_F\ {}_F\langle n|$ and $\sum_n |n\rangle_F\ {}_F\langle n+1|$. These operators are simple to handle since $|\psi\rangle_F$ is an eigenstate of both, with eigenvalue 1:

$$\sum_n |n+1\rangle_F\ {}_F\langle n|\,\psi\rangle_F = \sum_n |n\rangle_F\ {}_F\langle n+1|\,\psi\rangle_F = |\psi\rangle_F\,. \tag{B12}$$

Thus we can write:

$$\mathcal{H}_{OF}(t)\,|\psi\rangle_F = |\psi\rangle_F\left(\hat{O}e^{i\omega t} + \hat{O}^\dagger e^{-i\omega t}\right) = |\psi\rangle_F\,H_O(t) \tag{B13}$$

and also:

$$\begin{aligned}\mathcal{U}(t)\,|\psi\rangle_F &= \mathcal{P}\left[\exp\left[-i\int_0^t dt\left(\mathcal{H}_{sys} + \mathcal{H}_{OF}(t)\right)\right]\right]|\psi\rangle_F \\ &= |\psi\rangle_F\,\mathcal{P}\left[\exp\left[-i\int_0^t dt\left(H_{sys} + H_O(t)\right)\right]\right] = |\psi\rangle_F\,U(t)\end{aligned} \tag{B14}$$

which confirms Eq. (B11), and therefore completes the proof of the mapping.

To conclude this section, we note on the correspondence between the formalism presented above and the Floquet theorem

$$U(t) = W(t)\exp\left[-iH_F t\right] \tag{B15}$$

where $W(t+T) = W(t)$ and H_F is an operator acting on the system Hilbert space only, see main text, Eq. (4). The correspondence is given by noting that choosing $W(t=0) = \mathbb{I}$ gives

$$\exp\left[-iH_F t\right] = \langle\psi|_F\exp\left[-i\mathcal{H}_F t\right]|\psi\rangle_F \tag{B16}$$

1. Elimination of single photon processes

The auxiliery F-states formalism allows accounting for a sequence of virtual photon absorptions, by systematically eliminating the F-states associated with intermediate parts of the process. In the case we considered, for instance, there is no resonant single photon process. Therefore, if we start the system and F-state wave function with only an even number of photons, odd-photon F states will only appear with a suppressed amplitude since they have a large energy mismatch with the initial states of the wave function - they must be about an ω away.

Accounting for two-photon processes in our system is thus possible along the lines of ordinary second-order perturbation theory. We start by consdiering the propagator applied to the low-energy subspace, and read-off the effective hamiltonian that emerges after resumming connected diagrams. In our case, the low-energy subspace of the F-states is the superposition of all even states:

$$|\psi_{even}\rangle_F = \frac{1}{N'}\sum_n |2n\rangle_F\,. \tag{B17}$$

The effective two-photon propagator is then given by:

$$U(t) \approx U_2(t) =_F \langle\psi_{even}|\,\mathcal{U}(t)\,|\psi_{even}\rangle_F\,. \tag{B18}$$

Next, we need to expand the interaction Hamiltonian in powers of $\mathcal{H}_{OF}(t)$.

Before carrying out the expansion, let us move to the interaction picture of $\mathcal{H}_{sys}$ as well:

$$e^{i\mathcal{H}_{sys}t}U_2(t) \approx_F \langle\psi_{even}| e^{i\mathcal{H}_{sys}t}\mathcal{U}(t)|\psi_{even}\rangle_F =_F \langle\psi_{even}|\tilde{\mathcal{U}}(t)|\psi_{even}\rangle_F . \tag{B19}$$

with

$$\tilde{\mathcal{U}}(t) = \mathcal{P}\left[\exp\left(-i\int_0^t dt\tilde{H}_{OF}(t)\right)\right]. \tag{B20}$$

We denote

$$\tilde{\mathcal{H}}_{OF}(t) = e^{i(\mathcal{H}_{sys}+\mathcal{H}_\omega)t}\mathcal{H}_{OF}e^{-i(\mathcal{H}_{sys}+\mathcal{H}_\omega)t} = \sum_n \left(\hat{O}(t)|n+1\rangle_F\ {}_F\langle n| e^{i\omega t} + \hat{O}^\dagger(t)|n\rangle_F\ {}_F\langle n+1| e^{-i\omega t}\right). \tag{B21}$$

with $\hat{O}(t) = e^{i\mathcal{H}_{sys}t}\hat{O}e^{-i\mathcal{H}_{sys}t}$.

Now we are ready to expand the interaction Hamiltonian in powers of $\tilde{\mathcal{H}}_{OF}(t)$. Up to second order we encounter the terms:

$$\begin{aligned}\tilde{\mathcal{U}}(t) - 1 = -\int_0^t dt_2\int_0^{t_2} dt_1 \left(\hat{O}(t_2)|n+1\rangle_F e^{i(n+1)\omega t_2} + \hat{O}^\dagger(t_2)|n-1\rangle_F e^{i(n-1)\omega t_2}\right)\left({}_F\langle n|n\rangle_F e^{-in\omega(t_2-t_1)}\right)\\ \left(\hat{O}^\dagger(t_1)_F\langle n+1| e^{-i(n+1)\omega t_1} + \hat{O}(t_1)_F\langle n-1| e^{-i(n+1)\omega t_1}\right).\end{aligned} \tag{B22}$$

Note that we split the compound: $|n\rangle_F\ {}_F\langle m| e^{-i\omega(m-n)t} = |n\rangle_F e^{i\omega nt}\cdot_F\langle m| e^{-i\omega mt}$. The operators $\hat{O}, \hat{O}^\dagger$ could at this point be construed as *first quantized* operators, which change the state of a particle interacting with the radiation field.

Further progress is made by projecting on the initial, intermediate, and final states of the system described by $\mathcal{H}_{sys}$. Let us denote P_σ to be a projector of the system's state on the subspace of energy ϵ_σ. For now, we maintain the generality of the discussion, although eventually, we will restrict ourselves to $H_{sys} = H(\mathbf{k})$ which is a 4×4 Hamiltonian describing two 2d subspaces with energies $\pm\epsilon(\mathbf{k})$; at that point it will be simple to use $\sigma = \pm1$ to indicate the valence vs. conduction subspaces. Armed with this notation we can write:

$$\begin{aligned}\tilde{\mathcal{U}}(t) - 1 = -\sum_{\sigma_1,\sigma_2,\sigma_3}\int_0^t dt_2\int_0^{t_2} dt_1 P_{\sigma_3}\left(\hat{O}(t_2)|n+1\rangle_F e^{i(n+1)\omega t_2} + \hat{O}^\dagger(t_2)|n-1\rangle_F e^{i(n-1)\omega t_2}\right)P_{\sigma_2}e^{-in\omega(t_2-t_1)}\\ \left(\hat{O}^\dagger(t_1)_F\langle n+1| e^{-i\omega(n+1)t_1} + \hat{O}(t_1)_F\langle n-1| e^{-i\omega(n-1)t_1}\right)P_{\sigma_1}\end{aligned} \tag{B23}$$

This allows us to resolve the time dependence of the operators:

$$\begin{aligned}\tilde{\mathcal{U}}(t) - 1 = -\sum_{\sigma_1,\sigma_2,\sigma_3}\int_0^t dt_2\int_0^{t_2} dt_1 P_{\sigma_3}e^{-i(\epsilon_{\sigma_2}-\epsilon_{\sigma_3})t_2}\left(\hat{O}|n+1\rangle_F e^{i(n+1)\omega t_2} + \hat{O}^\dagger|n-1\rangle_F e^{i(n-1)\omega t_2}\right)P_{\sigma_2}\\ \left(\hat{O}_F^\dagger\langle n+1| e^{-i(n+1)\omega t_1} + \hat{O}_F\langle n-1| e^{-i(n-1)\omega t_1}\right)P_{\sigma_1}e^{-i(\epsilon_{\sigma_1}-\epsilon_{\sigma_2})t_1}e^{-in\omega(t_2-t_1)}\end{aligned} \tag{B24}$$

The expressions compactify by defining two indices $\mu_{1,2} = \pm1$, and denoting $\hat{O}^{(+1)} = \hat{O}^\dagger$ and $\hat{O}^{(-1)} = \hat{O}$, and dropping the subscript F,

$$\begin{aligned}\Delta\tilde{\mathcal{U}}(t) - 1 = -\sum_{\sigma_1,\sigma_2,\sigma_3}\sum_{\mu_1,\mu_2=\pm1}\int^t dt_2\int_{-\infty}^{t_2} dt_1 P_{\sigma_3}\hat{O}^{(-\mu_2)}\\ |n+\mu_2\rangle P_{\sigma_2}\hat{O}^{(\mu_1)}\langle n+\mu_1| P_{\sigma_1}e^{-i(\epsilon_{\sigma_1}-\epsilon_{\sigma_2})t_1 - i(n+\mu_1)\omega t_1}e^{-i(\epsilon_{\sigma_2}-\epsilon_{\sigma_3})t_2 + i(n+\mu_2)\omega t_2}e^{-in\omega(t_2-t_1)}\end{aligned} \tag{B25}$$

By moving to average time, $\bar{t} = \frac{t_1+t_2}{2}$ and time difference, $t_- = t_2 - t_1$, as well as integrating over t_- (while assuming that t is large and ignoring boundary terms for t_-, we get:

$$\tilde{\mathcal{U}}(t) - 1 = -\sum_{\sigma_1,\sigma_2,\sigma_3}\sum_{\mu_1,\mu_2=\pm1}\int d\bar{t}P_{\sigma_3}\hat{O}^{(-\mu_2)}|n+\mu_2\rangle P_{\sigma_2}\hat{O}^{(\mu_1)}\langle n+\mu_1| P_{\sigma_1}\frac{ie^{-i\bar{t}\left(\epsilon_{\sigma_1}-\epsilon_{\sigma_3}\right)}e^{-i\bar{t}\omega(\mu_1-\mu_2)}}{\frac{\epsilon_{\sigma_1}+\epsilon_{\sigma_3}}{2} + \omega\frac{\mu_1+\mu_2}{2} - \epsilon_{\sigma_2}} \tag{B26}$$

The time dependence on $\bar{t}$ is simply the interaction-representation time dependence. Therefore, by going back to the Schrödinger representation, we are able to get rid of the remaining time dependence in the expression, and we readily extract the effective second-order contributions to the effective $\mathcal{H}_F$:

$$\mathcal{H}^{eff}_{2-ph} = \sum_{\sigma_1,\sigma_2,\sigma_3}\sum_{\mu_1,\mu_2=\pm1}\sum_n |n+\mu_2\rangle_F\ {}_F\langle n+\mu_1|\frac{P_{\sigma_3}\hat{O}^{(-\mu_2)}P_{\sigma_2}\hat{O}^{(\mu_1)}P_{\sigma_1}}{\frac{\epsilon_{\sigma_1}+\epsilon_{\sigma_3}}{2} + \omega\frac{\mu_1+\mu_2}{2} - \epsilon_{\sigma_2}}, \tag{B27}$$

whereby now

$$\mathcal{H}_F^{eff} = \mathcal{H}_{sys} + \mathcal{H}_{2-ph}^{eff} + \mathcal{H}_\omega \tag{B28}$$

Again we note that $|\psi_{even}\rangle_F$ is an eigenstate with eigenvalue 1 of $\sum_n |n+\mu_2\rangle_{F\ F}\langle n+\mu_1|$ for $\mu_{1,2} = \pm 1$, which allows the mapping back to the original system. As before, the way to go back to the language of the original time dependent problem is to evaluate Eq. (B18), which yields

$$U_2(t) = \mathcal{P}\left[\exp\left[-i\int_0^t dt\left(H_{sys} + H_{2-ph}^{eff}(t)\right)\right]\right], \tag{B29}$$

with

$$H_{2-ph}^{eff}(t) = \sum_{\sigma_1,\,\sigma_2,\,\sigma_3}\ \sum_{\mu_1,\mu_2=\pm 1}\ \sum_n e^{i(\mu_2-\mu_1)\omega t}\frac{P_{\sigma_3}\hat{O}^{(-\mu_2)}P_{\sigma_2}\hat{O}^{(\mu_1)}P_{\sigma_1}}{\frac{\epsilon_{\sigma_1}+\epsilon_{\sigma_3}}{2}+\omega\frac{\mu_1+\mu_2}{2}-\epsilon_{\sigma_2}}, \tag{B30}$$

The form of Eq. (B30) is clearly in accord with degenerate perturbation theory. The reason for the putative degeneracy is the fact that we consider the energy of the F states representing the photons together with the energy of the system. A resonance, therefore, translates to a degeneracy in this language. It is interesting to note that Eq. (B27) generalizes degenerate perturbation theory to the case of near degeneracy. The energy denominator is actually the difference between the average of the initial and final energies, and the intermediate energy.

2. Application to the 3d FTI construction

Applying the formalism above to the 3d FTI construction is quite straightforward. We let $\hat{O} = \hat{O}^\dagger = \frac{1}{2}\hat{V} = \frac{1}{2}\vec{V}\cdot\vec{\gamma}$, and $P_\sigma = \frac{1}{2}\left(1+\sigma\frac{H(\mathbf{k})}{\epsilon_\mathbf{k}}\right)$ with $H(\mathbf{k}) = \bar{D}\cdot\vec{\gamma}$. We separate to two cases: (1) $\sigma_1 = \sigma_3$, $\mu_1 = \mu_2$, and (2)$\sigma_1 = -\sigma_3$, $\mu_1 = -\mu_2 = -\sigma_1$.

a. Case 1 - diagonal elements. The case of diagonal elements can be treated for both the valence and conduction band simultaneously, since terms that do not excite between the bands are time independent, and therefore the f terms factor out. Therefore:

$$\mathcal{H}_{\sigma_1=\sigma_3}^{eff} = |n\rangle_{F\ F}\langle n| \sum_{\sigma_1,\sigma_2=\pm 1,\,\mu=\pm 1}\frac{P_{\sigma_1}\frac{\hat{V}}{2}P_{\sigma_2}\frac{\hat{V}}{2}P_{\sigma_1}}{(\sigma_1-\sigma_2)\epsilon_\mathbf{k}-\mu\omega} \tag{B31}$$

Clearly $\sigma_2 = -\sigma_1$, otherwise the denominator makes the sum vanish. Thus:

$$\mathcal{H}_{\sigma_1=\sigma_3}^{eff} = |n\rangle_{F\ F}\langle n| \sum_{\sigma_1=\pm 1}\frac{P_{\sigma_1}\hat{V}P_{-\sigma_1}\hat{V}P_{\sigma_1}}{4\epsilon_\mathbf{k}^2-\omega^2}\cdot\sigma_1\epsilon_\mathbf{k} \tag{B32}$$

Elementary algebra of the Dirac matrices reduces this expression to:

$$\mathcal{H}_{\sigma_1=\sigma_3}^{eff} = |n\rangle_{F\ F}\langle n| \frac{\left(\vec{V}-\frac{1}{\epsilon_\mathbf{k}^2}\bar{D}\cdot\vec{V}\bar{D}\right)^2}{4\epsilon_\mathbf{k}^2-\omega^2}\frac{1}{2}\bar{D}\cdot\vec{\gamma} \tag{B33}$$

where we also recognize $\vec{V}_{\perp\hat{D}} = \vec{V} - \frac{1}{\epsilon_\mathbf{k}^2}\bar{D}\cdot\vec{V}\bar{D}$. Note that a term corresponding to Eq. (B33) also arises in the treatment involving the two rotating wave transformations. Consider the Hamiltonian $H_2(t)$, Eq. (A10), evaluated at values of $\mathbf{k}$ for which $2\omega = \epsilon(\mathbf{k})$, in the rotating wave approximation. For these $\mathbf{k}$ values, the terms $\varepsilon_+^{(1)}(\mathbf{k})P_+^{(1)}(\mathbf{k}) + (\varepsilon_-^{(1)}(\mathbf{k})+\omega)P_-^{(1)}(\mathbf{k})$ do not vanish, but give, to order $|\vec{V}_1|^2$ a term corresponding to Eq.(B33).

b. Case 2 - interband elements. The interband elements are to some extent more complicated, since we need to consider excitation and relaxation separately. We consider a term connecting the initial state σ_1 with $\sigma_3 = -\sigma_1$. For this process to be viable, we must have $\mu_1 = -\mu_2 = -\sigma_1$. Therefore, the specific term is:

$$\mathcal{H}_{\sigma_1\to-\sigma_1}^{eff} = |n+\mu_2\rangle_{F\ F}\langle n+\mu_1| \sum_{\sigma_2=\pm 1}\frac{P_{-\sigma_1}\frac{\hat{V}}{2}P_{\sigma_2}\frac{\hat{V}}{2}P_{\sigma_1}}{-\sigma\epsilon_\mathbf{k}} \tag{B34}$$

Using the form of P_{σ_2} we can carry out the sum, and obtain:

$$\mathcal{H}^{eff}_{\sigma_1\to-\sigma_1} = |n+\mu_2\rangle_{F\ F}\langle n+\mu_1| \frac{P_{-\sigma_1}\hat{V}H(\mathbf{k})\hat{V}P_{\sigma_1}}{-4\epsilon_k^2} \tag{B35}$$

Once again, elementary manipulations of the Dirac matrices yields:

$$\mathcal{H}^{eff}_{\sigma_1\to-\sigma_1} = \frac{1}{4}|n+\mu_2\rangle_{F\ F}\langle n+\mu_1| \left(-\frac{\vec{V}\cdot\bar{D}}{\epsilon_{\mathbf{k}}^2}\vec{V}_{\perp\hat{D}}\cdot\vec{\gamma} - \frac{\sigma_1}{2}\frac{\vec{V}\cdot\bar{D}}{\epsilon_{\mathbf{k}}^3}\left[\bar{D}\cdot\vec{\gamma},\vec{V}\cdot\vec{\gamma}\right]\right). \tag{B36}$$

This term seems indeed complicated. A simplification occurs, however, when we consider the RWA directly applied with a 2ω energy. The effective Hamiltonian connecting the two bands (that arises from V) is (the RWA eliminates the time dependence, and hence the F's):

$$\mathcal{H}^{eff}_{interband} = \mathcal{H}^{eff}_{1\to-1} + \mathcal{H}^{eff}_{-1\to1} = -\frac{\vec{V}\cdot\hat{D}}{2\epsilon_{\mathbf{k}}}\vec{V}_{\perp\hat{D}}\cdot\vec{\gamma} \tag{B37}$$

This term joins the direct two-photon process that arises from the $\vec{A}^2$ term appearing in D_5 due to the mass curvature. This term also coincides to second order in V, with the corresponding effect on the radiation-induced gap within the two consecutive rotating wave transformations. Note that at resonance $\epsilon_{\mathbf{k}} = 2\Delta\epsilon_{\mathbf{k}}$, and thus Eq. (B37) agrees with Eq. (A19).

[1] D. Hsieh, D. Qian, L. Wray, Y. Xia, Y. S. Hor, R. J. Cava, and M. Z. Hasan, Nature **452**, 970 (2008)
[2] Y. Xia, D. Qian, D. Hsieh, L. Wray, A. Pal, H. Lin, A. Bansil, D. Grauer, Y. S. Hor, R. J. Cava, and M. Z. Hasan, Nat Phys **5**, 398 (2009)
[3] H. Zhang, C.-X. Liu, X.-L. Qi, X. Dai, Z. Fang, and S.-C. Zhang, Nat Phys **5**, 438 (2009)
[4] A. M. Essin, J. E. Moore, and D. Vanderbilt, Physical Review Letters **102**, 146805 (2009)
[5] X.-L. Qi, R. Li, J. Zang, and S.-C. Zhang, Science **323**, 1184 (2009)
[6] L. Fu and C. Kane, Physical Review Letters **100**, 096407 (2008)
[7] T. Kitagawa, E. Berg, M. Rudner, and E. Demler, Physical Review B **82**, 235114 (2010)
[8] T. Kitagawa, M. S. Rudner, E. Berg, and E. Demler, Physical Review A **82**, 033429 (2010)
[9] T. Oka and H. Aoki, Physical Review B **79**, 081406 (2009)
[10] N. H. Lindner, G. Refael, and V. Galitski, Nature Phys. **7**, 490 (2011)
[11] Z. Gu, H. A. Fertig, D. Arovas, and A. Auerbach arXiv:1106.0302
[12] T. Kitagawa, T. Oka, A. Brataas, L. Fu, and E. Demler arXiv:1104.4636
[13] B. Dóra, J. Cayssol, F. Simon, and R. Moessner arXiv:1105.5963
[14] A. P. Schnyder, S. Ryu, A. Furusaki, and A. W. W. Ludwig, Physical Review B **78**, 195125 (2008)
[15] A. Kitaev, AIP Conf. Proc. **1134**, 22 (2009)
[16] X.-L. Qi, T. L. Hughes, and S.-C. Zhang, Physical Review B **78**, 195424 (2008)
[17] Z. Wang, X.-L. Qi, and S.-C. Zhang, New Journal of Physics **12**, 065007 (2010)
[18] In the following discussion we assume the absence of higher photon resonances, *i.e.*, $\omega > |D(\mathbf{k})|$. Multi photon resonances, do not affect our analysis in this manuscript, and we will consider their interesting effect in future work.
[19] L. Fu, C. L. Kane, and E. J. Mele, Physical Review Letters **98**, 106803 (2007)
[20] T. D. Stanescu, B. Anderson, and V. Galitski, Physical Review A **78**, 023616 (2008)
[21] Y. J. Lin, K. Jimenez-Garcia, and I. B. Spielman, Nature **471**, 83 (2011)
[22] S.-Y. Xu, L. A. Wray, Y. Xia, R. Shankar, A. Petersen, A. Fedorov, H. Lin, A. Bansil, Y. S. Hor, D. Grauer, R. J. Cava, and M. Z. Hasan arXiv:1007.5111
[23] S. Chadov, X. Qi, J. Kbler, G. H. Fecher, C. Felser, and S. C. Zhang, Nature Materials **9**, 541 (2010)
[24] H. Lin, L. A. Wray, Y. Xia, S. Xu, S. Jia, R. J. Cava, A. Bansil, and M. Z. Hasan, Nature Materials **9**, 546 (2010)
[25] D. Hsieh, F. Mahmood, J. W. McIver, D. R. Gardner, Y. S. Lee, and N. Gedik, Physical Review Letters **107**, 077401 (2011)
[26] D. Hsieh, J. W. McIver, D. H. Torchinsky, D. R. Gardner, Y. S. Lee, and N. Gedik, Physical Review Letters **106**, 057401 (2011)
[27] W.-K. Tse and A. H. MacDonald, Physical Review Letters **105**, 057401 (2010)
[28] V. M. Galitskii, S. Goreslavskii, and V. F. Elesin, Sov. Phys. JETP **30**, 117 (1970)
[29] L. I. Glazman, Sov. Phys. JETP **53**, 178 (1981)
[30] L. I. Glazman, Sov. Phys. Semi. **17**, 494 (1983)